NZNSEE PRESIDENT'S PAGE

It is my pleasure as your newly elected President to introduce myself. I am the Structural Engineering Group Leader at the Building Research Association of New Zealand (BRANZ) based at Judgeford, outside Wellington. I have been a member of the Management committee of the Society for the past 4 years and have now been honoured with the President's role. Members are probably aware that the Society's rules decree that the Presidential term is limited to two years, and from the experience of past presidents, this appears to be quite long enough.

I would like to thank your new editor, Les Megget, for this opportunity to provide a brief statement as to the current position of the Society and where I see us heading during my term as your President.

The issue foremost in the minds of your management committee is the 12th World Conference on Earthquake Engineering to be held in Auckland in January 2000. This is a major event both for New Zealand and the South Pacific and must be expected to involve considerable effort on all members of the Society. At this stage the conference committee has been formed under the chairmanship of Professor Bob Park. Planning is coming together with the task of hosting over 1200 delegates and with over 1500 papers expected setting the scene for a challenging but rewarding conference. During these early stages, much of the work will be undertaken by the Conference Committee themselves, but as the time approaches members should expect to be called on for assistance either with technical programme or for support in other areas. Please be generous with your time and reap the rewards of a successful conference.

The Societies technical study groups remain an area of strength. Several are in progress at this time including

- the Earthquake Risk Building Study Group, convened by David Brunsdon, are now focusing on pre-1976 Earthquake Prone Buildings with the support of the Building Industry Authority;
- the Industrial Plant Study Group, convened by Barry Davidson, has a positive endeavour to progress this group over the forthcoming year;
- the Storage Tanks Study Group is convened by Rob Jury and is looking towards developing a guide as to the seismic design of storage tanks as a supplement to the Red Book;
- the Post Earthquake Structural Response Study Group convened by Andrew Charleson has made considerable progress with its first phase of work and has distributed a to each Territorial Local Authority for comment as to how this work may be integrated into the TA's response plans;
- the Society also has taken an initiative to prepare a position paper on the need for Integrated Planning for Earthquake Preparedness during '96 which has been taken up by the secretary for Civil Defence and Internal Affairs and is being referenced by officials looking into the formulation of the Ministry of Emergency Management.

These Study Groups are a very effective way of bring the Societies collective expertise together to focus on topics of current interest and result in reports which are of direct and practical relevance to members. My thanks to each of the Study Group Convenors and to all members actively participating in these areas of development.

Maintaining public awareness of earthquakes and mitigation measures remains a clear focus of the Society and is expected to remain so over the forthcoming period. Planning is under way for our next annual conference (March 27/29 at Wairakei)

Andrew King

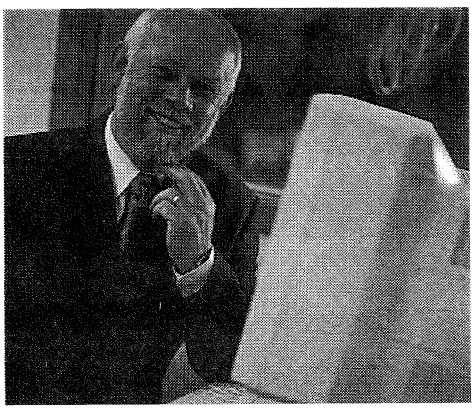

SEISMIC RESPONSE OF BRIDGE KNEE JOINTS HAVING COLUMNS WITH INTERLOCKING SPIRALS

J M Ingham[1], M J N Priestley[2] and F Seible[3]

ABSTRACT

A comprehensive laboratory investigation was conducted in which four large-scale structural concrete bridge knee joint units were tested. These units represented an as-built joint, and a repair, a retrofit, and a redesign of the as-built joint, and incorporated differing detailing including haunching, prestressing, and variations in the quantity of specially-placed joint reinforcement. Extensive experimental data led to an improved understanding of the force transfer mechanisms developed within joints of this type. A discussion of test unit response and a review of the most relevant data measured from each test are presented.

1. INTRODUCTION

While considerable attention has been given to both the interior and exterior beam-column joints of regular building frames, top-of-column joints found in the upper level of building frames have received significantly less attention, primarily as they carry little dead load relative to other joints within the frame. Of the previous investigations into building knee joint response, most have considered monotonic joint-opening or joint-closing actions only [1]. A limited amount of research has been conducted on the cyclic seismic response of beam-column knee joints, but again these investigations have focused on the detailing used in buildings [2-6].

The design of reinforced concrete bridges in the United States is now based upon the capacity design philosophy [7], requiring that joint damage be minimised during an earthquake so that structural collapse is prevented and subsequent joint repair is not required. However, the current United States concrete design code [8] and the regulatory document governing bridge construction [9] provide little direction in the design of such joints. Furthermore, guidelines provided in other design standards [10] are primarily derived for building frames, and result in excessive congestion of reinforcement when applied to bridge joints. Consequently, the development of a rational design procedure for reinforced concrete bridge joints is required.

Immediately following the Loma Prieta earthquake [11] a number of investigations considering the seismic response of reinforced concrete column-cap beam and column-footing connections were initiated. The research reported herein considered the in-plane (transverse) seismic response of bridge knee joints, and was prompted by the poor performance of outrigger bents from the San Francisco Bay Area. This investigation was complimented by a study conducted at the University of California at Berkeley, which considered the performance of bridge knee joints when subjected to out-of-plane forces developed in conjunction with longitudinal superstructure response [12].

Experimental investigation was conducted in the Charles Lee Powell structural systems laboratory at the University of California at San Diego in conjunction with an analytical study of knee joint response, based upon identifying the influence which differing reinforcement and geometric detailing have on joint force transfer mechanisms for both closing and opening actions applied to the joint [1].

This investigation considered a number of important aspects of bridge knee joint response not incorporated in previous studies. Large scale units were tested, and attention was given to the correct distribution of moments, shears, and axial forces acting at the joint boundaries. These aspects were of particular significance as both the reinforcement detailing and the distribution of forces in reinforced concrete bridge knee joints are generally much different from that found in the top-floor beam-column knee joints of regular building frames. Realistic modelling of prototype response allowed validation of a full-scale joint repair implemented in Oakland, California following the Loma Prieta earthquake, and a comprehensive assessment of reinforcement strain profiles aided in the identification of consistent joint force transfer mechanisms, leading to the formulation of a rational design procedure. Representative reinforcement strain data is reported, and it is noted that all data is in "customary" US units, accompanied by SI units in parenthesis.

[1] Department of Civil and Resource Engineering, University of Auckland (Member)

[2] Structural Systems Research Group, University of California at San Diego (Fellow)

[3] Structural Systems Research Group, University of California at San Diego

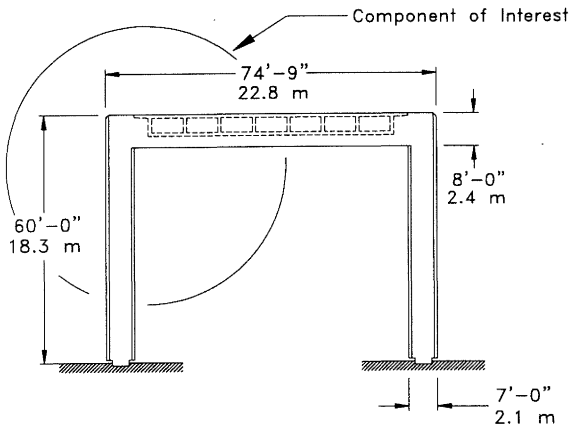

FIGURE 1 Dimensions of prototype structure.

2. PROTOTYPE RESPONSE AND MODELLING ISSUES

Test unit details were based on those of Bent 38 of the I-980 southbound connector in Oakland, California [13]. The general dimensions of the pin-based prototype are shown in Fig. 1, and damage to the structure sustained during the Loma Prieta earthquake is shown in Fig. 2. In Fig. 2a a number of cracks are clearly visible within the joint, oriented diagonally between the top outside corner and the re-entrant corner of the joint. Less distinct are a smaller number of joint cracks oriented in the orthogonal direction. In Fig. 2b a close-up of the embedded top cap beam reinforcement shows that one of these bars ruptured just prior to the 90° tail bend.

In regular building beam-column knee joints a total of 16-24 longitudinal reinforcement bars from both the beam and column are typically anchored in the joint. In reinforced concrete bridge knee joints it is not unusual to have as many as 60-80 longitudinal bars anchored in the joint, resulting in far greater detailing complexity. Consequently, the only way to realistically capture prototype response was through the use of test units satisfactorily large to preserve the appropriate joint detailing, reinforcement stress-strain characteristics, and typical geometric relationship between reinforcement size, and concrete aggregate size and crack widths.

The configuration of the adopted 1/3rd scale test set-up is shown in Fig. 3. While the prototype structure was a pin-based portal frame (see Fig. 1), only the top portion of the column was modelled in the laboratory, so that the unit required a moment-resisting footing. The footing, column, and cap beam and joint were cast in separate pours, resulting in a construction joint at the column-joint interface. The height of the column and the length of the cap beam were both selected to accommodate the seismic actuator, as shown. The lines of action of the seismic actuator and the loading jack replicating dead load forces both passed through a point on the column axis below the footing, representing the pin at the base of the prototype column.

Building beam-column knee joints generally support only light dead loading, which is legitimately neglected when testing the seismic response of sub-assemblies. The same is not true for bridge knee joints, where dead load force actions are typically of a similar magnitude to those associated with seismic response. Correct modelling of the appropriate force relationships has a considerable influence on the column axial force, and consequently the column plastic hinge strength. Similarly, it influences the cap beam shear force adjacent to the joint interface. For these reasons particular attention was given to the accurate modelling of both dead load and seismic forces acting at the joint boundaries.

Characteristic dead load and elastic seismic bending moment diagrams for the prototype structure are shown in Figs. 4a and

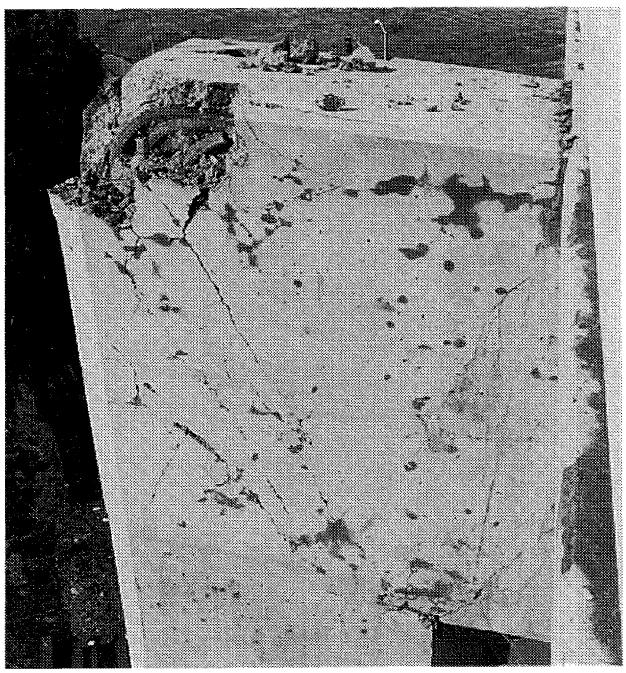

a, Elevation

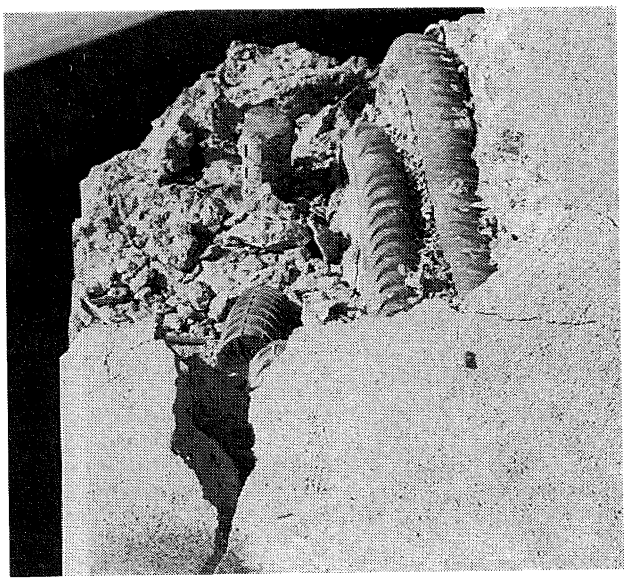

b, Plan

FIGURE 2 Damage to the prototype bent following the Loma Prieta Earthquake.

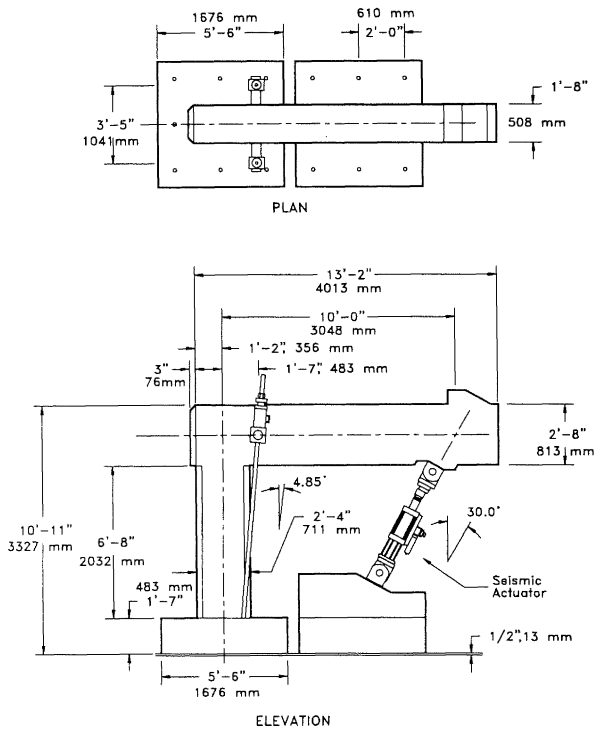

FIGURE 3 Configuration of test set-up.

4b. Figs. 4c and 4d show the corresponding bending moment diagrams developed in the test unit for both dead load and seismic actions. As the design philosophy for the retrofitted and redesigned units required elastic cap beam response, it was not necessary to model cap beam dead load bending moments away from the joint boundaries (see Fig. 4c). By modelling the prototype column bending moment diagram for both dead load and seismic force actions, column plastic hinge characteristics were effectively captured.

3. JOINT PERFORMANCE - CONCEPTUAL CONSIDERATIONS

The characteristic crack pattern developed in a knee joint subjected to closing actions is shown in Fig. 5a, accompanied by diagrams illustrating the forces acting at the joint boundaries and the corresponding orientation of joint shear stresses and joint principal tension stresses. Similarly, Fig. 6 shows the characteristic crack pattern developed in a knee joint subjected to opening actions, and the corresponding orientation of joint stresses.

When considering Figs. 5a and 6a it is evident that for both directions of joint loading a joint diagonal strut is developed. For joint-closing actions this strut is supported by the cap beam and column flexural compression stress resultants at the re-entrant corner of the joint, and by the reinforcement bend at the top outside corner of the joint, so that the strut and tie representation shown in Fig. 7a is appropriate for simple cases where there is no specially-placed joint reinforcement or joint prestress forces [1]. However, the stability of this mechanism is significantly influenced by the radius of the reinforcement bend so that care is required when dimensioning this detail.

For simple knee joints which are subjected to joint-opening actions and which have no specially-placed joint reinforcement or prestress forces, the strut and tie representation of Fig. 7b is

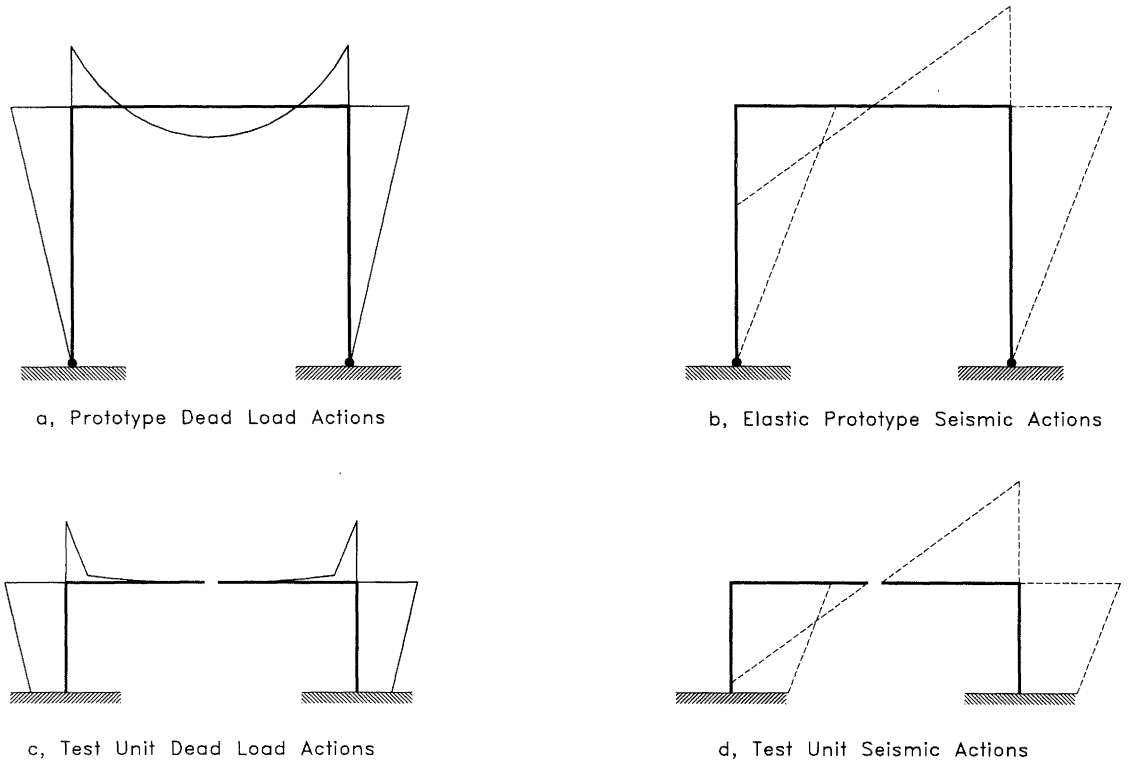

FIGURE 4 Prototype and test unit bending moment diagrams.

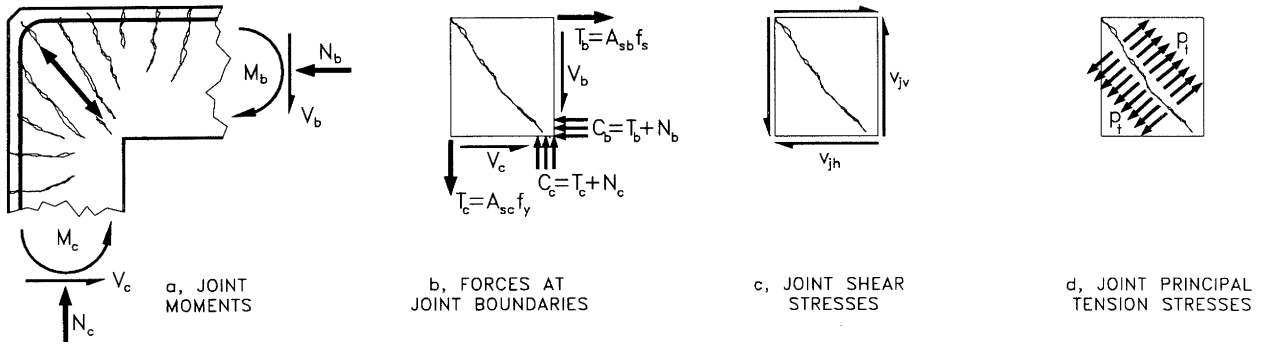

FIGURE 5 ***Diagonal tension stresses in a closing knee joint [after 14].***

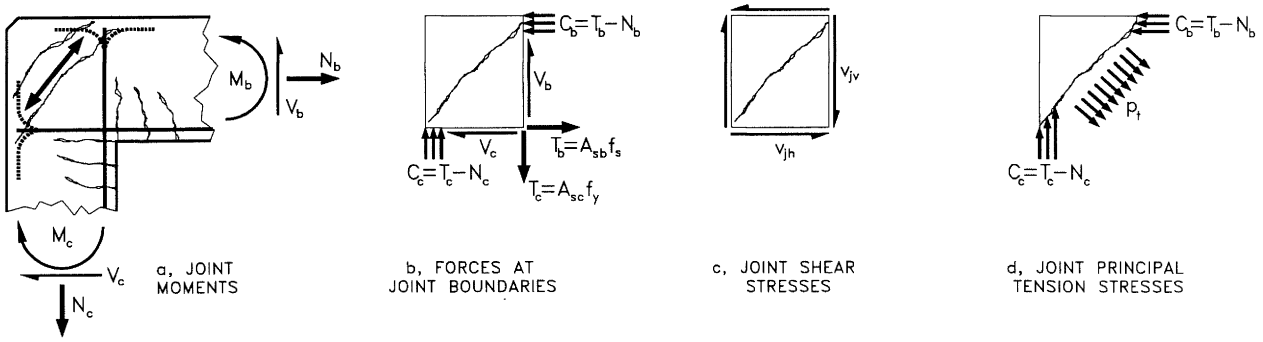

FIGURE 6 ***Diagonal tension stresses in an opening knee joint [after 14].***

appropriate, but again joint stability is partially dictated by reinforcement detailing. Fig. 6a shows column and cap beam longitudinal tension reinforcement anchored in the joint region. If the anchorage is provided by straight development length, it is unlikely that the necessary forces will be available to equilibrate the horizontal and vertical component of the diagonal strut at the lower and upper nodes (see Fig. 7b). If the tension reinforcement is anchored by hooks bent back into the joint (shown by dashed lines in Fig. 6a), conditions for anchoring the diagonal strut are generally improved. However, this detail, although desirable, is almost unbuildable, and inward bends on the column reinforcement are almost never used. The option of bending the heads away from the joint (also shown by dashed lines in Fig. 6a) is sometimes used, but is clearly even worse than straight anchorage in terms of supporting the diagonal strut.

By comparing the observed joint crack pattern developed in the prototype structure during the Loma Prieta earthquake (see Fig. 2a) with the joint-closing and joint-opening crack patterns shown in Figs. 5a and 6a it can be readily determined that the prototype joint sustained significant damage when subjected to closing actions. Also of interest was rupture in the prototype structure of the embedded top longitudinal cap beam reinforcement prior to the tail bend, with associated spalling of cover concrete at this location (see Fig. 2b), although it has been noted [15] that brittle failure of large diameter bent bars can occur at very low additional strain levels.

The discussion thus far has considered simple knee joints whose details are not specifically representative of the bridge joints considered in this investigation. However, more advanced joint force transfer mechanisms can be related directly to these simple mechanisms. Fig. 8 shows a representation of a mechanism which may be developed when the longitudinal member reinforcement does not utilise the full available embedment depth. The representation shown in Fig. 8 depicts the approximate depth of the various struts developed in the mechanism, which is clearly similar to the strut and tie model of Fig. 7b, except that demand is placed upon the transverse member reinforcement located adjacent to the joint. Also, additional demand is placed on longitudinal tension reinforcement at the joint boundaries to equilibrate the outward struts D_1 and D_2. This implies a reduction in tension force

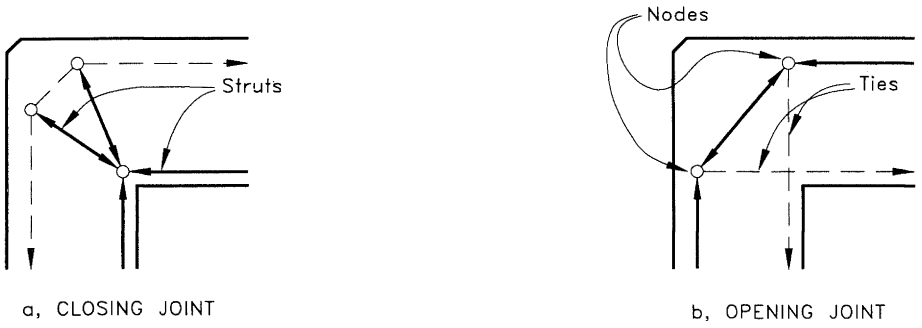

FIGURE 7 ***Fundamental knee joint strut and tie models.***

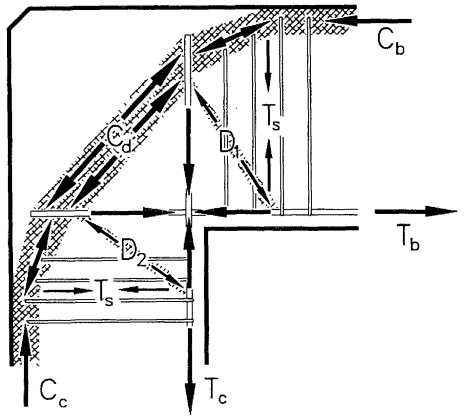

FIGURE 8 Member-assisted joint opening mechanism [1].

capable of resisting applied moments at the joint boundaries.

Additional joint force transfer mechanisms relevant to this investigation, which are again extensions to the fundamental response indicated in Fig. 7, are the haunched joint force transfer mechanisms of Fig. 9 and the prestress joint force transfer mechanisms of Fig. 10, which are both shown as distributed force models rather than their strut and tie equivalent to more clearly illustrate the variations in strut geometry. Fig. 9 indicates that when using a joint haunch the depth of the joint diagonal strut can be expected to increase, which will improve reinforcement embedment conditions when subjected to joint-opening actions. Similar response is also developed when the joint is prestressed (see Fig. 10), where the joint diagonal strut will form as a fan, being supported by the prestress anchors acting on the back face of the joint. More complete discussion of these joint force transfer mechanisms is available in [1].

4. TEST UNIT DETAILS

4.1 As-built unit

The as-built unit had details representative of the prototype structure, with a column comprised of longitudinal reinforcement located within two interlocking spirals as shown in Fig. 11a, and a cap beam with a comparatively low longitudinal reinforcement ratio in the bottom of the section (see Fig. 11b). The prototype structure was designed using elastic procedures, resulting in the cap beam positive (joint opening) moment capacity being significantly less than the column positive moment capacity as the column strength was dictated by reinforcement placed to support negative (joint closing) moments. It is noted that using current capacity design procedures, column plastic hinges are required to form adjacent to bridge knee joints under both opening and closing actions, resulting in less damage to the bridge superstructure and reduced repair difficulty.

The joint reinforcement details of the as-built unit are shown in Fig. 12a. Most notably, the transverse column reinforcement (ρ_s = 0.92%) was not extended into the joint, but was instead replaced by a horizontal joint spiral having a significantly reduced diameter (ρ_s = 0.07%). Similarly, the cap beam longitudinal side reinforcement and the cap beam transverse reinforcement were terminated at the joint interface, effectively resulting in no specially-placed reinforcement within the joint

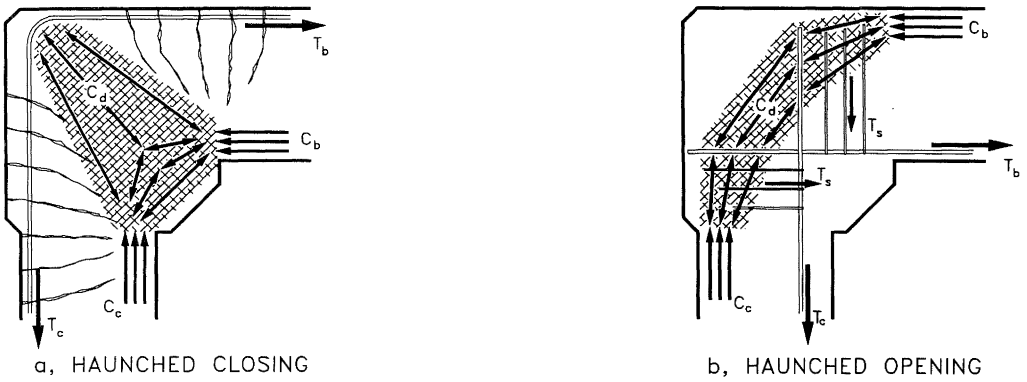

FIGURE 9 Haunched joint force transfer mechanisms.

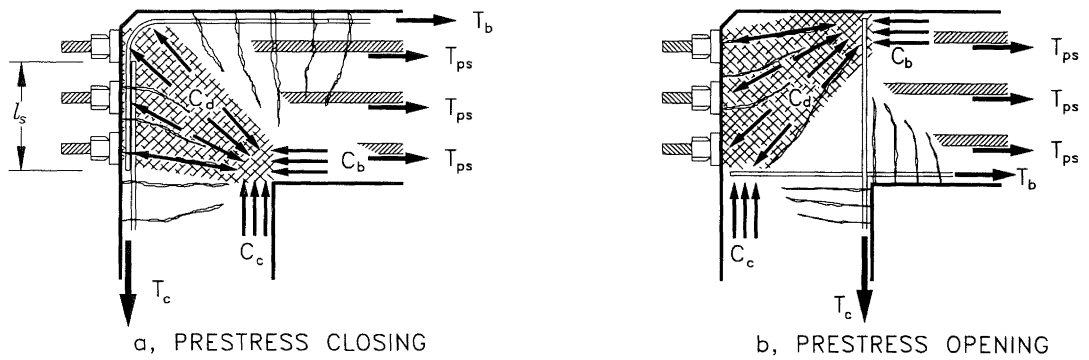

FIGURE 10 Prestress joint force transfer mechanisms.

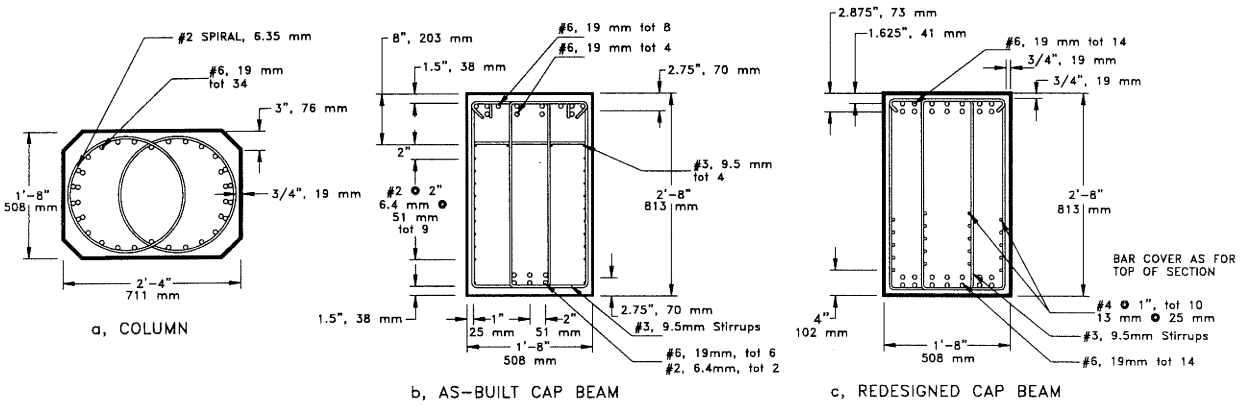

FIGURE 11 Member section details.

region. Multiple 90° tails from the top cap beam reinforcement were lap spliced to bundled longitudinal column reinforcement without effective horizontal joint reinforcement to confine the splice. As bundled bars were spliced, larger shearing stresses were generated than for a conventional unconfined lap splice. Also relevant was the radius of the 90° bend, which was approximately three times greater than the code required minimum [8], aiding in the support of a joint diagonal strut when subjected to closing actions (see Figs. 5a and 7a).

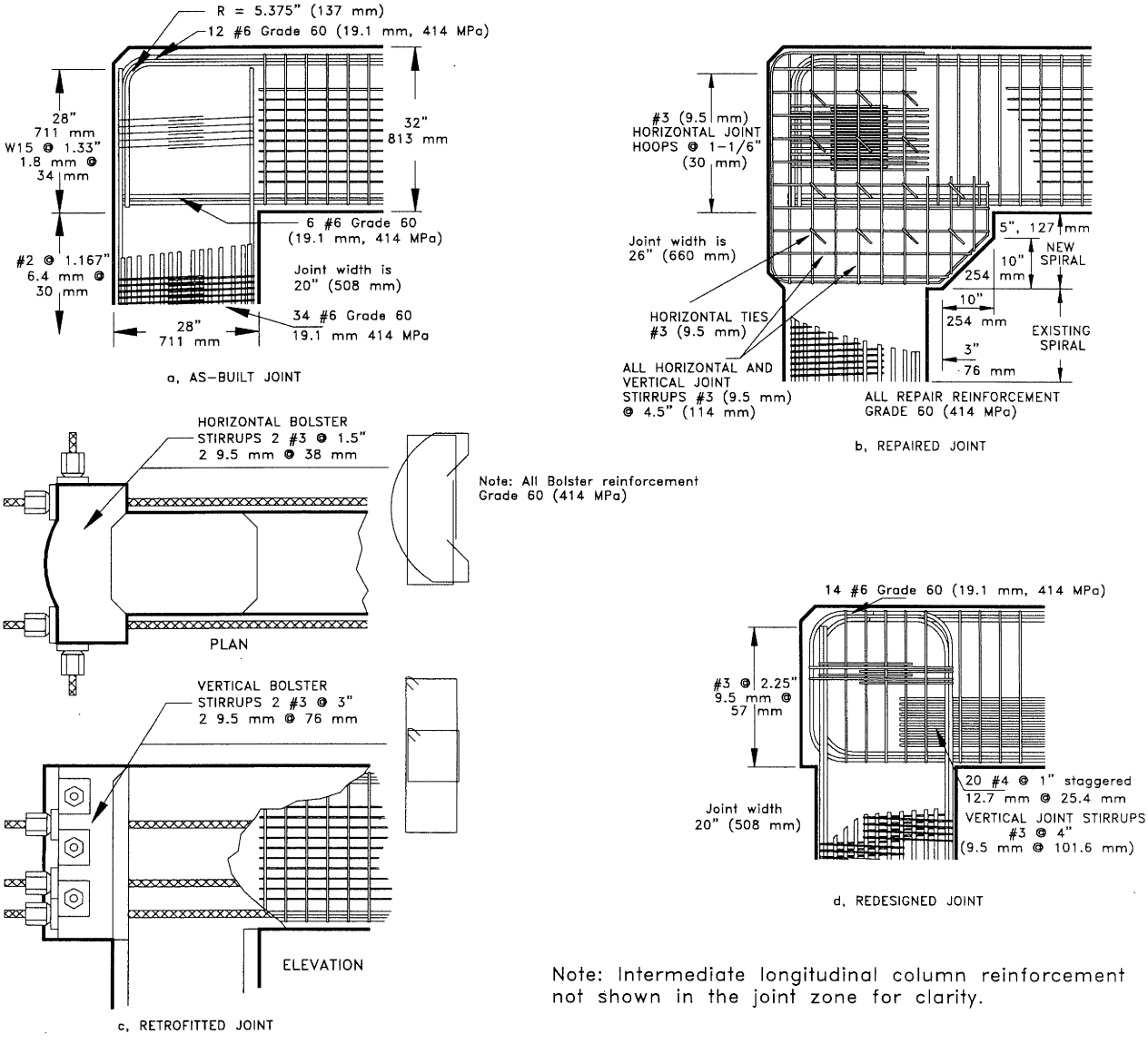

FIGURE 12 Details of four bridge knee joint units having columns with interlocking spirals.

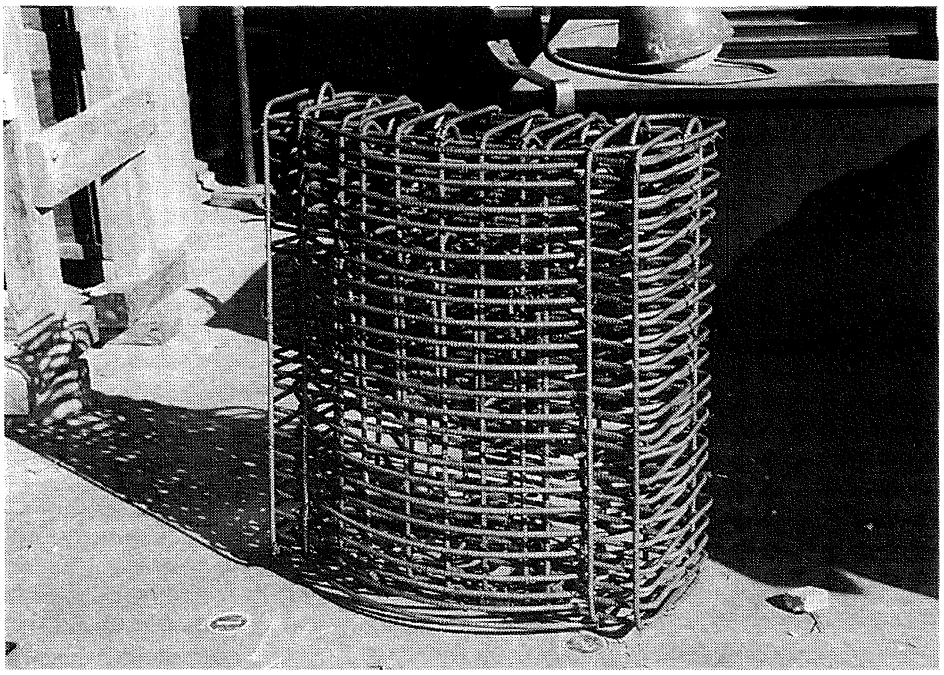

FIGURE 13 Prefabricated bolster reinforcement cage.

4.2 Repaired unit

Following failure of the as-built unit (described subsequently), displacements were returned to zero and the cap beam supported. All the concrete of the joint core was removed and new specially-designed joint reinforcement was added. The repair to the laboratory unit was similar to the prototype joint repair, and included a joint haunch as shown in Fig. 12b, effectively increasing the embedment length of the longitudinal member reinforcement (see Fig. 9). The width of the joint was increased from 20 inches (508 mm) to 26 inches (660 mm), proportionally reducing the magnitude of the maximum joint stresses. Although the test unit joint repair was representative of the prototype repair, the quantity of specially-placed joint reinforcement was higher in the test unit to ensure elastic joint response.

The quantity of specially-placed horizontal reinforcement in the repaired joint was based upon the requirements of the then-current New Zealand code of practice for the design of concrete structures [16]. The most severe joint demand corresponded to the formation of a column plastic hinge for joint-closing actions, with the cap beam tension reinforcement approaching its yield strength. Consequently the maximum horizontal joint shear force was (see Fig. 5):

$$V_{jh} = A_{sb} f_y \qquad (1)$$

and assuming concrete shear mechanisms to be ineffectual, the required area of horizontal joint reinforcement (using the same reinforcement grade) was:

$$A_{jh} = \frac{V_{jh}}{f_y} = A_{sb} = 12 \times 0.44 = 5.28\,\text{in}^2 \left(3406\,\text{mm}^2\right) \qquad (2)$$

The joint reinforcement details of the repaired unit are shown in Fig. 12b. Interlocking joint hoops were placed up the full column reinforcement embedment length, supporting the lap splice between the column reinforcement and the vertical tails of the top cap beam reinforcement. The joint hoops were surrounded by a grid of horizontal and vertical joint stirrups, with horizontal ties added to prevent out-of-plane joint dilation. Using the details shown in Fig. 12b, the provided horizontal joint reinforcement was:

$$A_{jh} = 0.11 \times 2 \times \frac{\pi}{4} \times \frac{28}{1.17} + 0.11 \times 2\text{x}\frac{28}{4.5} = 5.52\,\text{in}^2 \left(3561\,\text{mm}^2\right)$$

which was 5% more than required by Eq. 2. Cap beam side reinforcement was extended into the joint, but cap beam stirrups again terminated at the original joint interface.

4.3 Retrofitted unit

Elastic joint response was measured when the repaired unit was tested, but as expected, inelastic cap beam response developed when the unit was subjected to joint-opening actions. Consequently a retrofit strategy was adopted which utilised external prestressing of the cap beam and joint as shown in Fig. 12c, addressing deficient aspects of the two previous units. A nominally-identical companion to the as-built unit was constructed, with the outer face of the as-built joint roughened and dowels set into the joint core to provide stability to the reinforcement cage of the bolster, which anchored the external prestress tendons. The bolster reinforcement cage consisted of both horizontal and vertical stirrups sets (see Fig. 12c) and was prefabricated before being lifted into position (see Fig. 13).

By applying an eccentric prestress force, T_{ps}, of 600 kips (2667 kN), the flexural strength of the cap beam was sufficiently elevated to ensure column plastic hinging for both directions of loading. The prestress force provided a confining pressure to the lap splice between the longitudinal column reinforcement and the vertical tails of the top cap beam reinforcement, and also provided hook restraint for the top cap beam reinforcement, preventing opening of the 90° hooks for applied joint-closing actions.

The cap beam and joint prestress force of the retrofitted unit resulted in a reduced joint principal tension stress, p_t:

$$p_t = \left(\frac{p_x + p_y}{2}\right) - \sqrt{\left(\frac{p_x - p_y}{2}\right)^2 + v_j^2} \qquad (3)$$

but an increased joint principal compression stress, p_c:

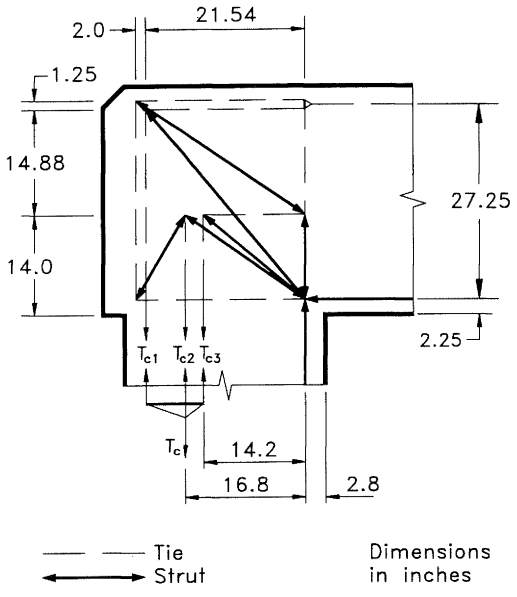

Note:
Location of member flexural stress resultants determined from section analyses

FIGURE 14 Depiction of force transfer mechanisms assumed when redesigning for joint-closing actions.

$$p_c = \left(\frac{p_x + p_y}{2}\right) + \sqrt{\left(\frac{p_x - p_y}{2}\right)^2 + v_j^2} \qquad (4)$$

when compared with the non-prestressed equivalent, where p_x and p_y are the average direct compression stresses in the joint region in the horizontal and vertical directions respectively, and v_j is the average joint shear stress. Due to the adopted retrofit strategy the depth of the joint diagonal strut was increased in response to both the distribution of prestress anchors on the back face of the joint, and to the increased depth of the cap beam flexural compression stress resultant (see Fig. 10). Consequently, the retrofit strategy also provided improved anchorage for the embedded longitudinal column reinforcement.

To support anchorage of the external longitudinal prestress tendons discussed above, the bolster was stressed in the orthogonal out-of-plane direction (see Fig. 12c), which had the beneficial effect of providing more uniform bearing upon the back face of the as-built joint. However, to ensure that the bolster remained nominally elastic the beneficial influence provided by this out-of-plane bolster prestressing was neglected when detailing the horizontal bolster stirrups. Assuming diagonal struts oriented at approximately 45° from the prestress anchors to the back face of the as-built joint, the required area of Grade 60 horizontal joint stirrups, having a probable yield strength of 67 ksi (462 MPa), was:

$$A_{bh} = \frac{0.5 \times T_{ps} \tan 45°}{f_y} = \frac{0.5 \times 600}{67} = 4.48\,\text{in}^2 \left(2890\,\text{mm}^2\right) \qquad (5)$$

while the provided reinforcement area (see Fig. 12c) was:

$$A_{bh} = 2 \times 0.11 \times \frac{32}{1.5} = 4.69\,\text{in}^2 \left(3026\,\text{mm}^2\right)$$

Additional bolster details have been previously reported [17].

4.4 Redesigned unit

For the redesigned unit the basic geometry and the width of the as-built joint were retained, but the reinforcement of the cap beam and joint was redesigned (see Figs. 11c and 12d) in accordance with the capacity design procedure [14] to ensure that column plastic hinging would develop during an earthquake. This resulted in a small increase in top longitudinal cap beam reinforcement and a considerable increase in bottom longitudinal cap beam reinforcement. The distribution of longitudinal reinforcement in the redesigned cap beam (see Fig. 11c) was primarily dictated by the as-built distribution of longitudinal column reinforcement (see Fig. 11a), recognising that a total of 82 longitudinal bars were embedded in the joint region. The vertical tails of the top and bottom cap beam reinforcement were continuous within the joint and small joint stub, and horizontal tails were provided to twelve longitudinal column reinforcing bars located near the inside face of the section (see Fig. 12d).

Joint reinforcement comprised of multiple sets of interlocking hoops distributed up the full height of the joint, and oblong hoops enclosing both the embedded longitudinal column reinforcement and the connected vertical tails of the embedded top and bottom longitudinal cap beam reinforcement. Vertical joint reinforcement was uniformly distributed across the joint, and vertical hook restraint was provided to the horizontal tails of the appropriate longitudinal column reinforcement.

A column flexural tension force [18] accounting for strain-hardened overstrength was adopted:

$$T_c = \left(0.5A_{sc}\right) \times \left(1.3f_y\right) \qquad (6)$$
$$= 0.5 \times 34 \times 0.44 \times 1.3 \times 67 = 651.5\,\text{kips}\ \left(2898\,\text{kN}\right)$$

where a probable yield strength of f_y = 67 ksi (462 MPa) was assumed. The cap beam longitudinal reinforcement was designed to approach its yield strength as column hinging developed. As an example, for joint-closing actions (see Fig. 14) the corresponding cap beam flexural tension force was:

$$T_b = \frac{651.5 \times 16.8}{27.25} = 401.7\,\text{kips}\ \left(1787\,\text{kN}\right)$$
$$= 0.97A_{sh}f_y$$

The design procedure for joint-closing actions was based upon recognising that several mechanisms aided in supporting the column flexural tension force, T_c:

Mechanism C1: A component T_{c1} was transferred directly across the lap splice between the column reinforcement and the inner vertical tails of the connected top and bottom cap beam reinforcement (see Fig. 12d), requiring confinement of the lap splice;

Mechanism C2: A component T_{c2} was supported by struts oriented both towards the re-entrant corner and towards the bottom tail bend of the outer cap beam reinforcement in the joint stub;

Mechanism C3: A component T_{c3} was tied into the diagonal joint strut using horizontal joint hoops.

These three mechanisms are together depicted in Fig. 14.

Based upon experimental data obtained from a second series of tests reported elsewhere [19], it was assumed that the connected vertical tails of both sets of top and bottom cap beam reinforcement would support $0.75f_y$, with $0.25f_y$ being transferred to the joint core by bond stresses, primarily at the top tail bend. Consequently the component of the column flexural tension force, T_c, to be supported by Mechanism C1 was:

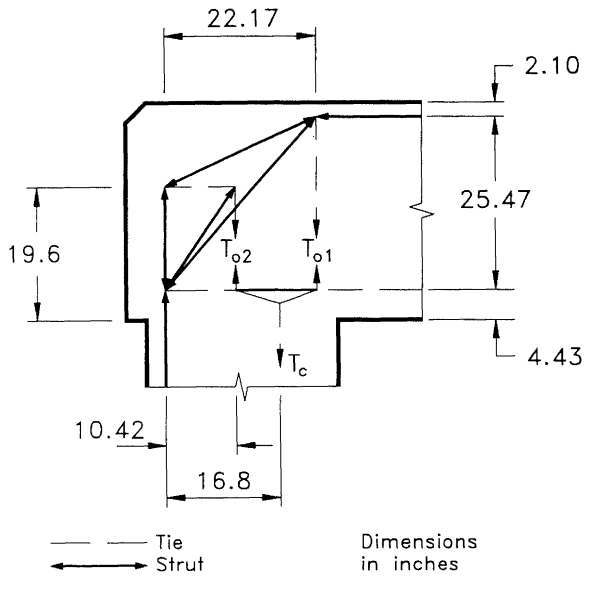

Note:
Location of member flexural stress resultants determined from section analyses

FIGURE 15 Depiction of joint force transfer mechanisms assumed when redesigning for joint-opening actions.

$$T_{c1} = A_s f_s = 7 \times 0.44 \times (0.75 \times 67) = 154.8 \text{ kips } (688.6 \text{ kN})$$

requiring a confining stress across the lap splice [18] of:

$$f_t = \frac{154.8}{\mu_f \ell_s D'} = \frac{154.8}{1.4 \times 20.0 \times 18.25} = 0.303 \text{ ksi } (2.09 \text{ MPa}) \quad (7)$$

Assuming #3 (9.5 mm) grade 60 (414 MPa) joint hoops (see Fig. 12d), the required hoop spacing was:

$$s = \frac{A_s f_y}{f_t D'} = \frac{2 \times 0.11 \times 67}{0.303 \times 18.25} = 2.66 \text{ in. } (68 \text{ mm}) \quad (8)$$

and the provided hoop spacing (see Fig. 12d) was 1.125 in. (29 mm), indicating that the lap splice was sufficiently confined.

Based upon developing $0.75f_y$ in the outer vertical tails of the connected top and bottom cap beam reinforcement located in the small joint stub, the component of the column tension force to be resisted by Mechanism C2 was (see Fig. 14):

$$T_{c2} = \frac{154.8 \times 23.54}{16.8} = 216.9 \text{ kips } (965 \text{ kN})$$

so that the component supported by Mechanism C3 was:

$$T_{c3} = T_c - T_{c1} - T_{c2}$$
$$= 651.5 - 154.8 - 216.9 = 279.8 \text{ kips } (1245 \text{ kN})$$

which acted at a lever-arm of:

$$\bar{x} = \frac{651.5 \times 16.8 - 154.8 \times (21.54 + 23.54)}{279.8} = 14.2 \text{ in. } (361 \text{ mm})$$

For joint-closing actions reinforcement strain data indicated that a uniform distribution of bond stress was developed along the embedded column reinforcement, explained by recognising that minimal transverse tension strain was developed at this location. For the adopted detailing, no bond distress was observed when the repaired, retrofitted and redesigned units were subjected to joint-closing actions, so that a limiting bond stress for this design case was not established. Assuming satisfactory bond, the joint force required to tie T_{c3} into the joint diagonal strut (see Fig. 14) was:

$$F_h = \frac{T_{c3}\bar{x}}{(0.5\ell_a - 2.25)} = \frac{79.8 \times 14.2}{0.5 \times 28.0 - 2.25} = 338.1 \text{ kips } (1504 \text{ kN})$$

and using the joint hoop details described earlier, the required spacing was:

$$s = \frac{0.11 \times 2 \times 67 \times 28.0}{338.1} = 1.22 \text{ in. } (31 \text{ mm})$$

When redesigning for joint-opening actions, the column flexural tension force given by Eq. 6 was again adopted. Recognising that twelve longitudinal column bars were provided with horizontal tail bends (see Fig. 12d), it was assumed that a component of the column tension force, T_c (see Eq. 6) of:

$$T_{o1} = 12 \times 0.44 \times 67 = 353.8 \text{ kips } (1574 \text{ kN})$$

was transferred directly to the joint diagonal strut (see Fig. 6a and Fig. 15). Also, due to the presence of large transverse tension strains from the embedded bottom cap beam reinforcement, poor bond conditions were developed along the lower portion of the embedded column reinforcement. For this reason $0.4\ell_a$ located adjacent to the joint boundary was assumed to be ineffectual in providing reinforcement anchorage. The remaining component of the column flexural tension force of:

$$T_{o2} = 651.5 - 353.8 = 297.7 \text{ kips } (1324 \text{ kN})$$

which acted at a lever-arm of:

$$\bar{x} = \frac{651.5 \times 16.8 - 353.8 \times 22.17}{297.7} = 10.4 \text{ in. } (265 \text{ mm})$$

was therefore supported over a length of $0.6\ell_a$ adjacent to the end of the bar in a region of transverse compression strain, resulting in satisfactory bond transfer [1]. Consequently, for the geometry shown in Fig. 15 a horizontal joint force of:

$$F_h = \frac{297.7 \times 10.4}{(0.7 \times 28.0 - 4.43)} = 204.1 \text{ kips } (908 \text{ kN})$$

was required to tie T_{o2} into the joint diagonal strut, and using the detailing described earlier, a reinforcement spacing of:

$$s = \frac{0.11 \times 2 \times 67 \times 0.6 \times 28}{204.1} = 1.21 \text{ in. } (31 \text{ mm})$$

was required, which corresponded closely with the spacing required for joint-closing actions.

4.5 Material properties

The material properties of the concrete and reinforcement used in this test program accurately represented the material characteristics of the prototype structure, and the measured strengths are reported in Table 1 and Table 2 respectively. A super-plasticiser admixture was added on site when placing the joint concrete of the repaired unit, and when placing the joint and cap beam concrete of the redesigned unit.

4.6 Instrumentation

Each test unit was instrumented with a large number of devices used to measure displacements, rotations, curvatures, and joint-deformations, allowing the deformed shape of the unit to be accurately determined. Also, a comprehensive distribution of reinforcement strain gauges were mounted on reinforcement primarily located within the joint region, which was beneficial in the identification of representative joint force transfer mechanisms. A more thorough description of the instrumentation has been provided elsewhere [17].

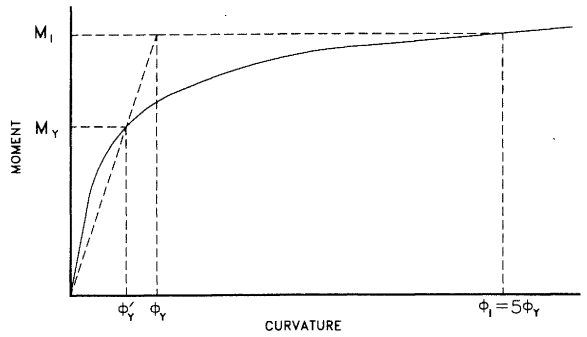

Note: ϕ_Y is referred to as the bilinear yield curvature

FIGURE 16 Definition of the ideal moment.

4.7 Application of test forces and displacements

The testing history required identifying the critical flexural member framing into the joint for both joint-closing and joint-opening seismic actions. Ideal member strength was calculated using measured material strengths (ϕ=1) and was defined as shown in Fig. 16 to eliminate a dependency upon the ultimate concrete compression strain, ε_{cu}, and indirectly a dependency upon section detailing. Thus ideal moment capacity, M_i, corresponded to the theoretical flexural strength at a curvature of $5\phi_y$, where ϕ_y was defined as the nominal yield curvature. The nominal yield curvature, ϕ_y, was found by extrapolation of the straight line from the origin through the moment M_y and curvature ϕ'_y corresponding to first yield, to the ideal moment, M_i. Actuator forces corresponding to first yielding of the member longitudinal reinforcement (F_y) and to development of the member ideal moment (F_i) were then identified.

In the majority of tests the additional joint-closing dead load force necessary to replicate prototype dead load actions was applied incrementally and simultaneously offset by a joint-opening seismic actuator force, so that zero moment was maintained at the column-joint interface. Consequently, cyclic testing was not begun at zero actuator force but at zero column moment, which corresponded to a seismic actuator force of approximately +25 kips (+111 kN). A standardised sign convention was adopted, with joint-opening termed the positive direction for moments, seismic actuator forces, and vertical cap beam displacements. Consequently, joint-closing moments, seismic actuator forces, and vertical cap beam displacements were negative.

Unit type	As-built	Repaired	Retrofitted	Redesigned
Column	5310 (36.6)	5310[4] (36.6)	5500 (37.9)	5340[5] (36.8)
Joint	4390 (30.3)	4630 (31.9)	6670 (46.0)	7370 (50.8)
Cap beam	4390 (30.3)	4390 (30.3)	6670 (46.0)	7370 (50.8)
Bolster	—	—	4180 (28.8)	—

TABLE 1 Measured day of test concrete strengths, psi (MPa).

[4] Measured strength of as-built unit reproduced as true strength not measured.

[5] Upper 12 in. (305 mm) of column as per joint.

Following application of the seismic actuator force required to provide zero column moment at the joint interface, the seismic actuator was cycled to force limits of approximately $\mp F_y/4$, $\mp F_y/2$ and $\mp 3F_y/4$. The last cycle was completed five times, representing the maximum serviceability loading condition. Next, a single force cycle to $\mp F_y$ was completed, and the bilinear yield displacement was determined by linearly extrapolating the measured displacement Δ'_y to the ideal moment conditions. That is:

$$\Delta_y = \Delta'_y \frac{M_i}{M_y} \qquad (9)$$

Note that this generally resulted in different yield displacements for the two directions of loading. Following force-controlled testing, displacement-controlled testing was conducted with three cycles to $\mu_\Delta = \mp 1$, $\mu_\Delta = \mp 1.5$, $\mu_\Delta = \mp 2$, $\mu_\Delta = \mp 3$, and finally five cycles to the maximum displacement limits of the seismic actuator.

5. EXPERIMENTAL RESULTS

5.1 As-built unit

Joint cracking developed in a fan pattern as progressively larger joint-closing actions were applied to the as-built unit (see Figs. 5a and 17a), and during the first semi-cycle to $-F_y$ extensive diagonal splitting occurred within the joint. This splitting developed due to failure of the unconfined lap-splice between the vertical tails of the top cap beam reinforcement and the embedded longitudinal column reinforcement (see Fig. 12a), and resulted in the significant strength loss identifiable in Fig. 18a. With repeated cycling there was further physical and strength degradation of the joint, with extensive spalling of the joint cover concrete occurring at the top outside corner (see Fig. 17b), corresponding closely to the observed damage to the prototype structure following the Loma Prieta earthquake (see Fig. 2a).

The formation of joint-opening cracks was delayed with respect to that observed for joint-closing actions due to a corresponding reduction in the joint principal tension stress (see Eq. 3), recognising the greatly reduced tension input to the joint for a

Unit type	As-built	Repaired	Retrofitted	Redesigned
#6 long. Column	68.9 (475)	68.9 (475)	66.1 (455)	62.5 (431)
#2 trans. column	49.6 (342)	49.6 (342)	52.0 (346)	48.9 (337)
#6 long. cap beam	72.9 (502)	72.9 (502)	64.4/62.7 (444/432) top/bottom	62.5 (431)
add long. cap beam	#3 (9.5) 82.2 (566)	#3 (9.5) 82.2 (566)	#3 (9.5) 65.3 (450) #2 (6.4) 62.1 (428)	#4 (12.7) 69.3 (477)
#3 trans. cap beam	82.2 (566)	82.2 (566)	65.3 (450)	67.2 (463)
horiz. joint	W15 (1.8) not recorded	#3 (9.5) not recorded	W15 (1.8) not recorded	67.2 (463)
#3 bolster	—	—	66.8 (460)	—

TABLE 2 Measured reinforcement strengths, ksi (MPa).

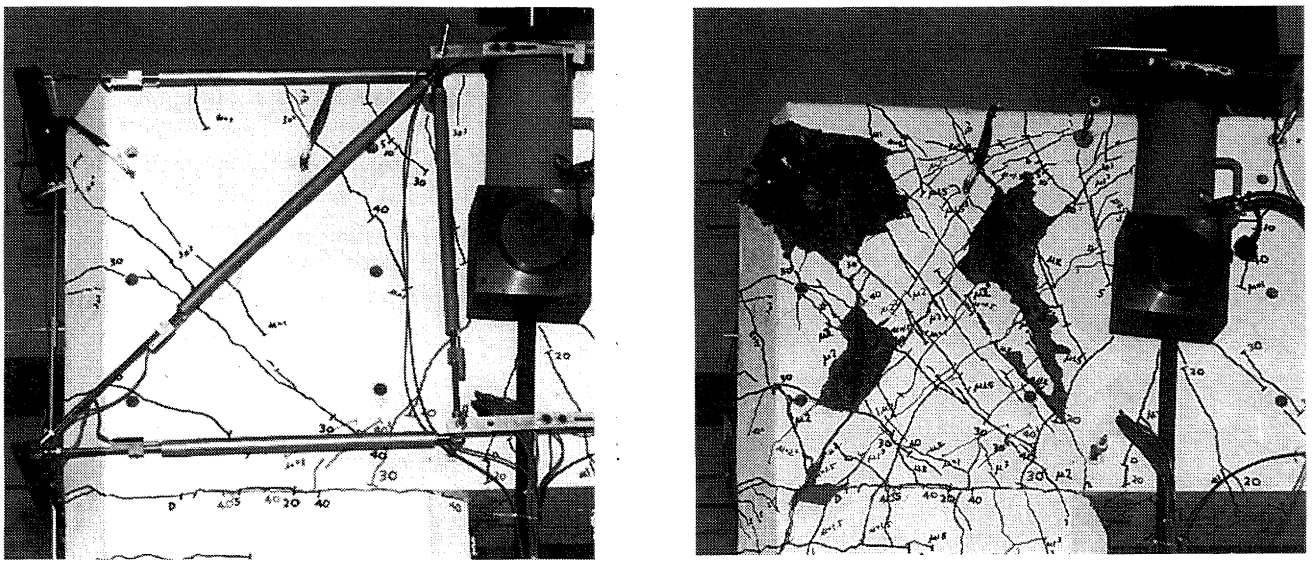

a) Joint failure prior to first yielding

b) End of test

FIGURE 17 As-built unit during testing.

cap beam plastic hinge (see Fig. 11b). However, joint cracking due to opening actions did develop at μ_Δ = 1.2, corresponding to a joint principal tension stress of $3.5\sqrt{f_c'}$ (psi) or $0.29\sqrt{f_c'}$ (MPa). Partly based upon these observations, it has been suggested [7,18] that for bridge knee joints in which the joint principal tension stress does not exceed the limits noted above, only nominal specially-placed joint reinforcement is required. In addition a joint strength degradation model has been suggested for unreinforced joints, which in the majority of cases will exhibit a failure mode similar to the as-built unit, rather than failure by alternative modes such as strut-crushing. This degradation model, whose descending branch was matched to the test result, is shown in Fig. 19.

Recognising that prior to the decay of joint integrity the lap splice failure occurring for joint-closing actions should not influence joint-opening response, the low measured strength of the as-built unit for joint-opening actions (see Fig. 18a) supported the force transfer mechanism shown in Fig. 8, where the member flexural stress resultants have a reduced lever-arm at the joint interfaces, resulting in reduced section flexural strength.

5.2 Repaired unit

When joint-closing seismic actuator forces were applied to the repaired unit, the cap beam and column cracks previously formed during testing of the as-built unit reopened. At the end of the test full joint cracking had developed, similar to the pattern shown in Fig. 5a, but these cracks were narrow, indicating that the joint reinforcement had not yielded. A column plastic hinge developed, with spalling of the column cover concrete on the inside face of the section (see Fig. 20).

Little joint cracking due to opening actions developed prior to μ_Δ = 3.0, at which time a large number of arch cracks developed within the repaired joint. These arch cracks, which had an almost vertical orientation at the column-joint interface, became increasingly horizontal closer to the cap beam-joint interface (see Fig. 20), so that their geometry was different to that developed in the as-built unit (see Fig. 17b). Arching of the cracks in the reinforced joint of the repaired unit was due to the presence of joint reinforcement [7] and improved anchorage of the embedded column reinforcement.

Testing of the repaired unit was terminated when first one, and then the remaining five longitudinal bars in the bottom of the cap beam section (see Fig. 11b) ruptured at the joint interface at μ_Δ = 3.6. However, due to the large area of longitudinal reinforcement in the top of the cap beam section there was no crushing or spalling of the cap beam cover concrete. It was because of this plastic hinge that the ideal moment definition shown in Fig. 16 was selected, which is independent of the ultimate concrete compression strain, ε_{cu}. Of particular note is that the measured strength of the cap beam was in excellent agreement with pre-test predictions (see Fig. 18b). This was attributed to the influence of the joint haunch (see Fig. 9b), resulting in the location of the cap beam flexural stress resultant at the joint interface being consistent with standard flexural theory, rather than exhibiting a reduced lever-am as for the cap beam plastic hinge of the as-built unit (see Fig. 8). Strain data measured along the embedded longitudinal column reinforcement located adjacent to the inside face of the joint (see Fig. 21) supported formation of the force transfer mechanism recommended when designing for joint-opening actions, where negligible bond is assumed along the initial portion of the embedment length as discussed previously.

As a consequence of the elastic design procedure, unidirectional plastic hinging developed in the column for joint-closing actions, and in the cap beam for joint-opening actions (see Fig. 20). Moment-curvature histories for the two plastic hinge regions are shown in Fig. 22, clearly indicating the formation of these unidirectional hinges. Average strains in joint reinforcement did not exceed 85% of the yield strain, even at maximum response, indicating that the provisions of [16], based upon the requirements for joints in building frames, were overly conservative when applied to bridge joints.

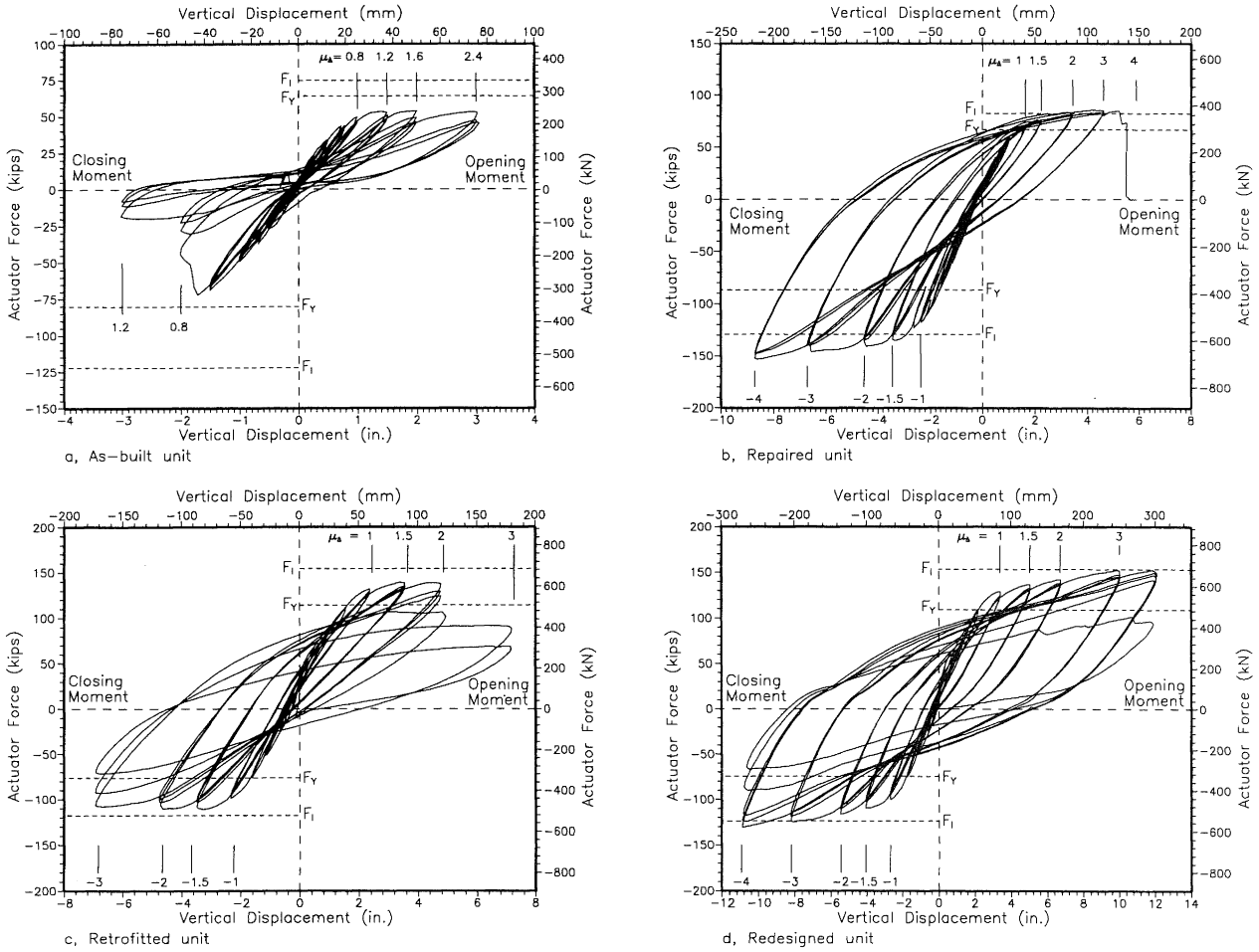

FIGURE 18 Force-displacement histories for four bridge knee joint units.

5.3 Retrofitted unit

When testing the retrofitted unit flexural cracking developed along the full length of the column for both joint-closing and joint-opening seismic actuator forces. Initially there was little cracking in the cap beam or joint due to the reduced principal tension stress (see Eq. 3), but when the joint-opening seismic actuator force corresponding to first yielding of the longitudinal column reinforcement (F_y) was reached, extensive joint cracking developed. Notably this pattern of cracking (see Fig. 23a) differed markedly from that observed for previous tests, corresponding closely with the assumed force transfer mechanism (see Fig. 10b). At $\mu_\Delta = 1.5$ there was crushing and spalling of column cover concrete at the joint interface, indicating the development of a column plastic hinge for both directions of loading. At this ductility level the measured strength of the unit approximately corresponded to pre-test predictions (see Fig. 18c).

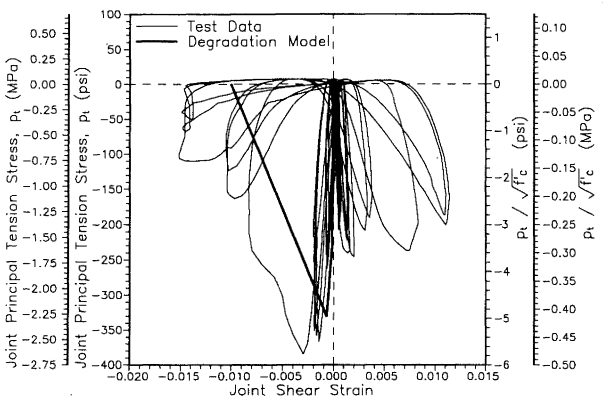

FIGURE 19 Joint principal tension stress history for the as-built unit.

Spalling of joint cover concrete began at $\mu_\Delta = 2$, with significant strength loss for joint-opening actions (see Fig. 18c). Less strength loss was noted for joint-closing actions, reflecting the geometry of the joint diagonal strut confined by both the cap beam and column flexural compression stress resultants at the reentrant corner of the joint (see Fig. 10a). With further cycling to a displacement ductility of $\mu_\Delta = 3$ there was continued deterioration of joint integrity (see Fig. 23b) and a corresponding loss in strength, and after three cycles to this ductility level the test was terminated.

Moment-curvature data confirmed that the prestressed cap beam remained elastic, and that prior to damage to the joint core a column plastic hinge was responsible for inelastic displacements for both directions of loading. Furthermore, there was no evidence of failure to the lap splice between the vertical tails of the top longitudinal cap beam reinforcement and the embedded longitudinal column reinforcement for closing actions applied to the joint.

The joint principal compression stress-shear strain history is shown in Fig. 24. Computed maximum joint principal compression stresses approximately corresponded with pretest

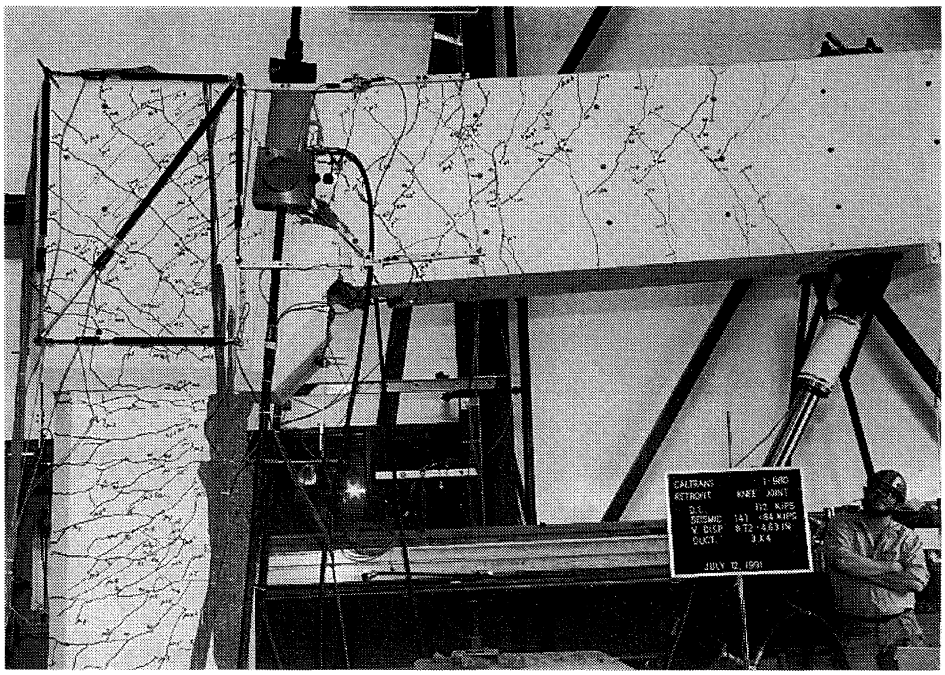

FIGURE 20 Repaired unit at maximum displacement.

predictions and were clearly too large to ensure satisfactory response of the effectively unreinforced joint. Following testing, this result was used to develop an assessment method to identify possible joint strut crushing [1]. It is recommended that assessment for this mode of failure be conducted during design, particular for joints having prestressed cap beams.

Cap beam stirrups located adjacent to the joint interface remained elastic for joint-closing actions (see Fig. 25a), but yielded during opening of the joint (see Fig. 25b) when the dead load and seismic shear forces acted in opposite directions and there was a reduced shear force at this location. This supported the joint-opening mechanism shown in Fig. 8 for unhaunched knee joints.

5.4 Redesigned unit

When testing the redesigned unit major flexural cracking developed in the column at early stages of the test, and after 5 cycles representing serviceability loading extensive joint cracking attributable to both joint-closing and joint-opening seismic actuator forces had developed, consistent with the high joint principal tension stress developed in the non-prestressed joint. Joint cracking which developed for actions opening the joint again formed an arch shape (see Fig. 26a), as for the repaired unit. At a displacement ductility of $\mu_\Delta = 1.5$ there was limited crushing and spalling of cover concrete at the column-

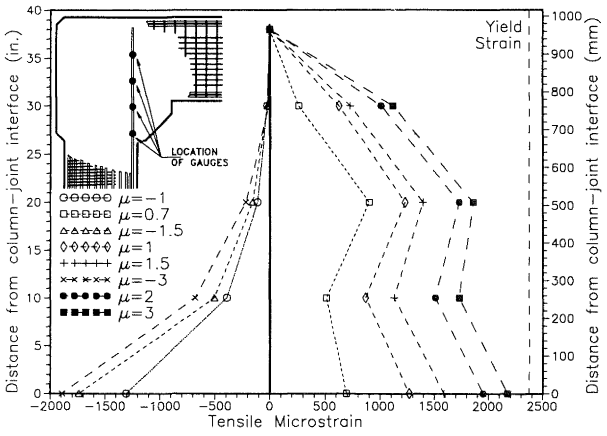

FIGURE 21 Strain profiles along embedded column reinforcement of the repaired unit (see inset for location of gauges).

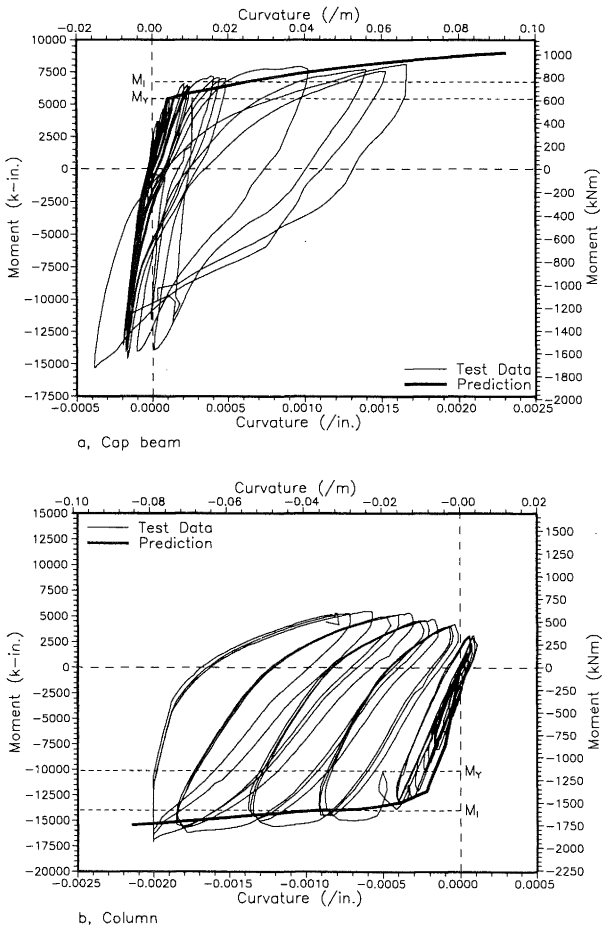

FIGURE 22 Moment-curvature histories for the unidirectional hinges of the repaired unit.

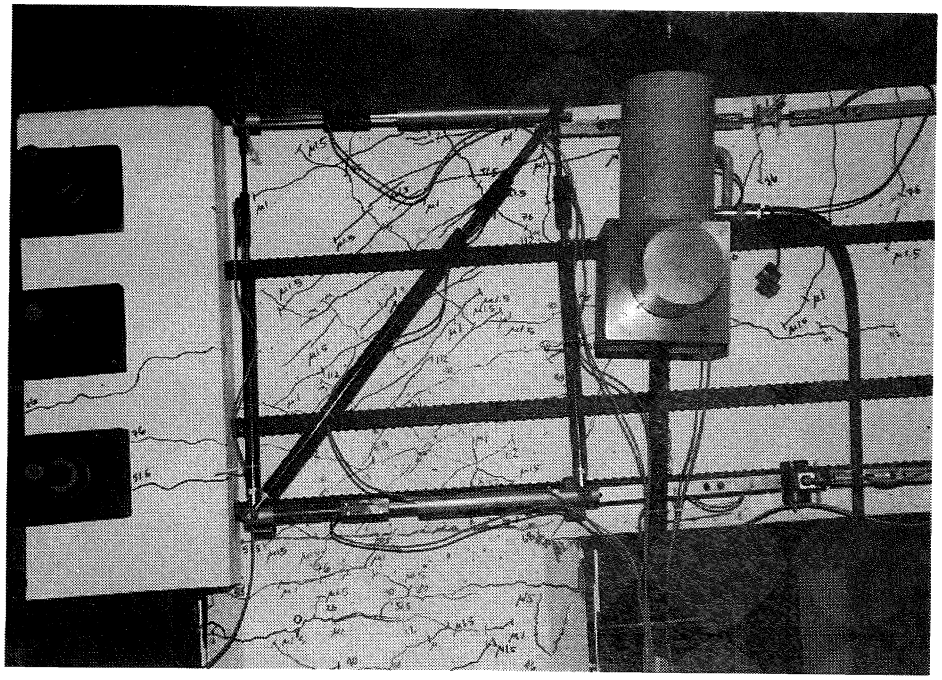

a) Joint crack pattern after cycling at ductility 1.5

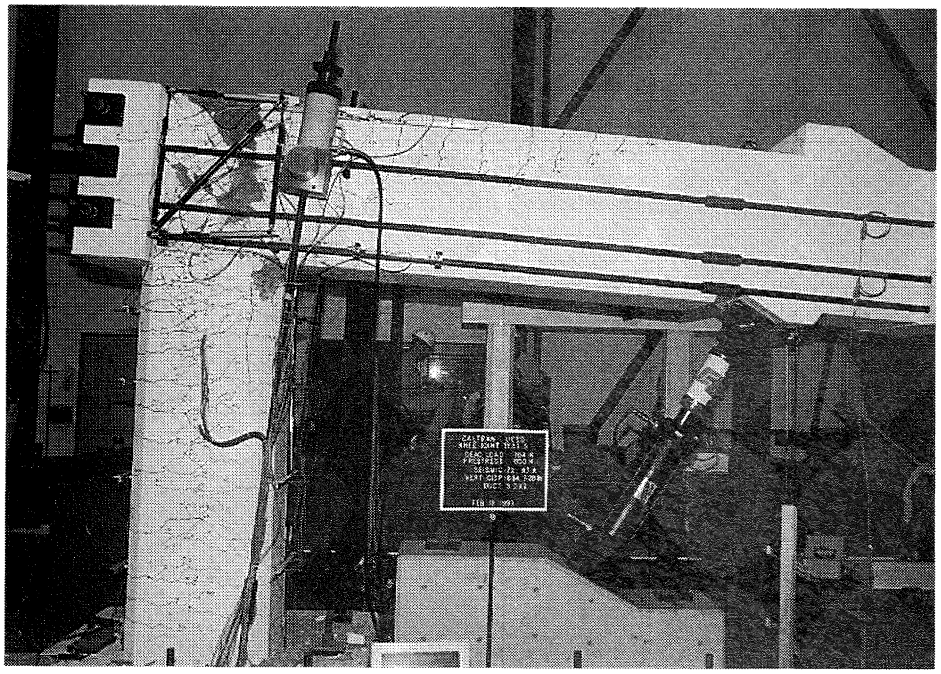

b) Unit at end of test

FIGURE 23 Retrofitted unit at different stages of testing.

joint interface, suggesting the formation of a column plastic hinge. This was followed by limited spalling of joint cover concrete at displacement ductility $\mu_\Delta = 2$.

After three cycles to the maximum range of the actuator there was yielding of the transverse column reinforcement in the plastic hinge region, followed by buckling and then rupture of the longitudinal column reinforcement in the plastic hinge region in subsequent cycles. Similar to behaviour noted previously for tests on columns with interlocking spiral [20], this pattern of transverse column reinforcement resulted in a satisfactory plastic hinge, and the measured strength of the unit was in excellent agreement with pre-test predictions (see Fig. 18d). Fig. 26b shows the test unit at the end of the test. Notably, targeted response was achieved despite extensive spalling of joint cover concrete, the development of inelastic joint deformations [17], and maximum joint shear stresses of $14\sqrt{f_c'}(\text{psi})$ or $1.16\sqrt{f_c'}(\text{MPa})$, in excess of the applicable US design standards [8, 9].

Measured strain data confirmed that a significant proportion of the column flexural tension stress resultant which developed for

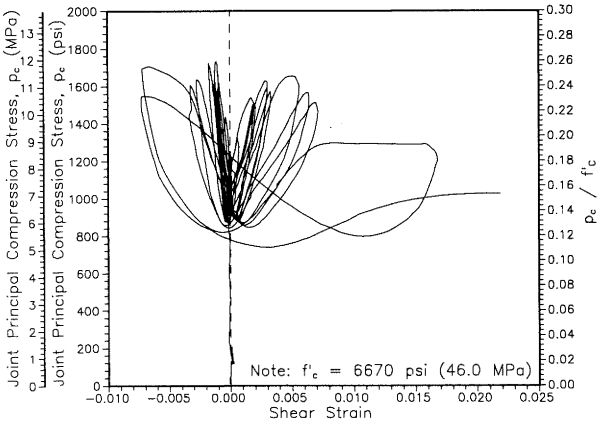

FIGURE 24 ***Joint principal compression stress history for the retrofitted unit.***

actions opening the joint penetrated to the height of the horizontal tails (see Fig. 12d), and was consequently transferred directly to the joint diagonal strut. Similarly, strain data confirmed that the cap beam flexural tension stress resultant which developed for closing actions penetrated to the vertical tail at the back of the joint, and even to a portion of the bottom longitudinal cap beam reinforcement, as shown in Fig. 27. Most importantly, strain data confirmed that the majority of specially-placed joint reinforcement approached or slightly exceeded its yield strain, validating the rational design procedure described previously.

5.5 Comparison of measured response

In Fig. 28 the force-displacement envelopes of the four units are plotted. When comparing these envelopes it is necessary to recognise that the haunched joint of the repaired unit resulted in relocation of the critical flexural section for both directions of loading and that for actions opening the joint, the cap beam was the critical flexural member for the as-built and repaired units and the column was the critical flexural member for the retrofitted and redesigned units.

From Fig. 28 it can be determined that the repaired, retrofitted, and redesigned units all had significantly improved response when compared to the as-built unit. For joint-closing actions the envelope for the repaired unit shows the greatest strength due to its relocated critical flexural section, but the envelope for the redesigned unit indicates the greatest inelastic displacement capacity. For joint-opening actions the influence of haunching the joint, prestressing the cap beam, and redesigning the cap beam are clearly evident, with the redesigned unit again supporting the greatest inelastic displacement. It can also be identified that by prestressing the joint and cap beam, the retrofitted unit had a notably stiffer cracked-section initial stiffness for joint-opening actions than did the non-prestressed redesigned unit.

6. CONCLUSIONS AND RECOMMENDATIONS

6.1 Background

1. The reinforcement details used in bridge knee joints are typically very different from those used in building beam-column knee joints. Previous research on the seismic response of building beam-column knee joints is not directly relevant when investigating bridge knee joint response.
2. The poor response of outrigger bents in the Loma Prieta earthquake revealed the need for research into the seismic response of bridge knee joints.
3. Experimental data collected during testing of large scale units was beneficial when formulating strut and tie models.

6.2 As-built unit

1. Response observed in the laboratory matched that observed in the field, validating the test set-up.
2. Poor response can be expected when knee joints having an effectively unconfined lap splice between the embedded longitudinal tension reinforcement of the cap beam and column are subjected to joint-closing actions.
3. The maximum joint principal tension stress is an appropriate parameter for assessing the extent of probable joint cracking. For bridge knee joints effectively having no specially-placed joint reinforcement, joint cracking can be expected to significantly influence response.
4. For closing actions applied to effectively unreinforced joints, member reinforcement tension strains can be expected to penetrate to the top outside corner of the joint.

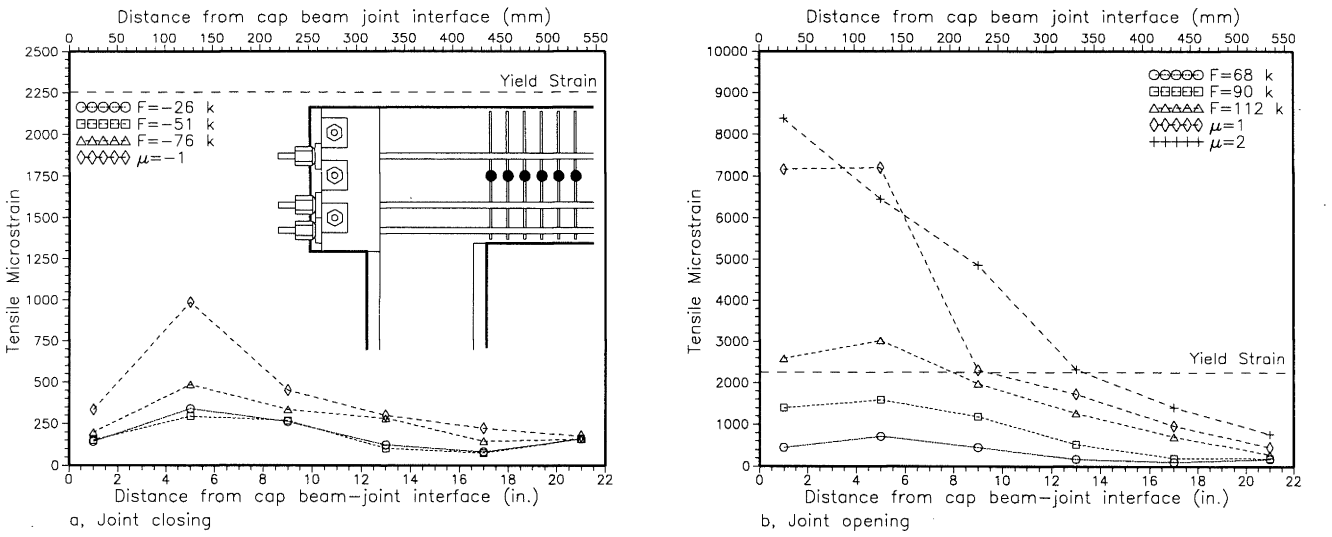

FIGURE 25 ***Strain profiles from transverse cap beam reinforcement of the retrofitted unit (see inset for location of gauges).***

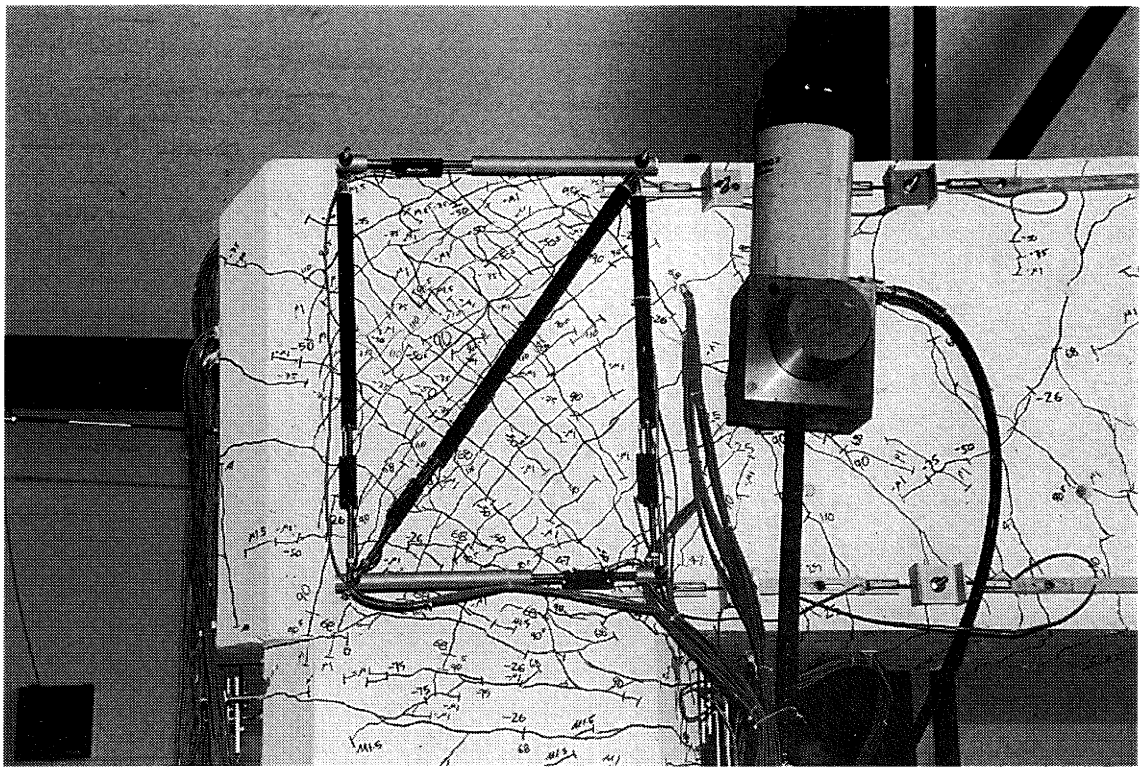

a) Details of joint crack pattern

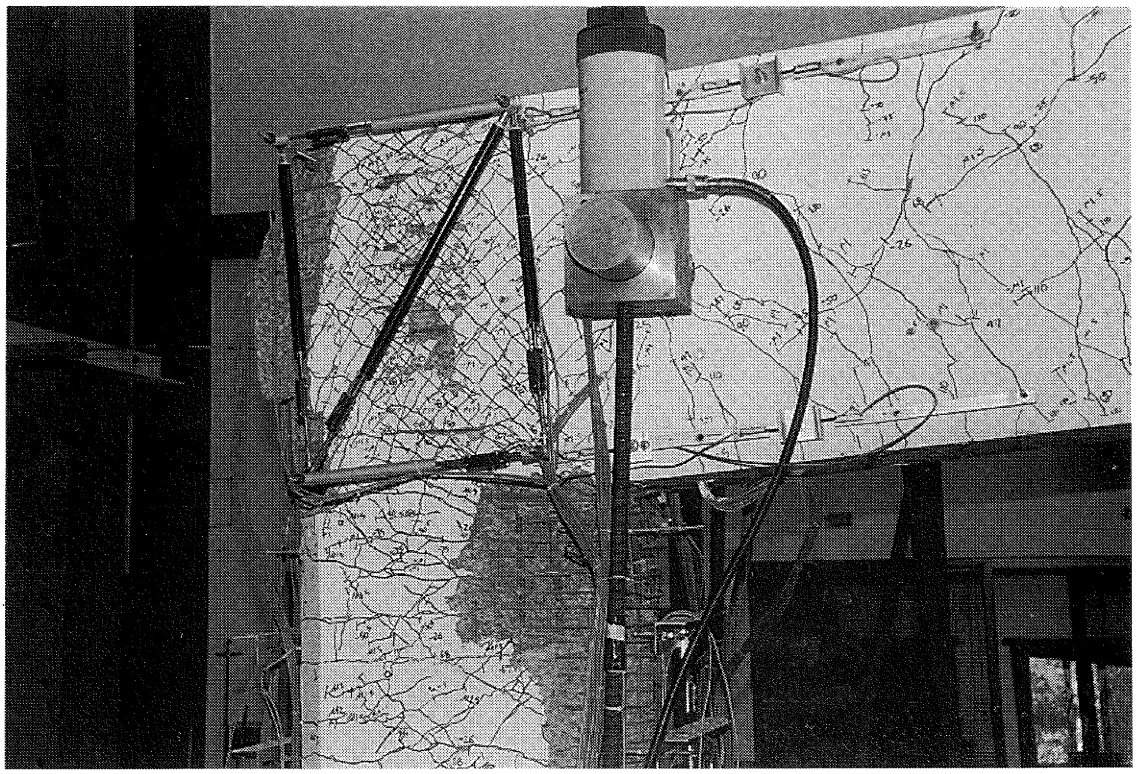

b) Redesigned unit at end of test

FIGURE 26 Redesigned unit during testing.

5. Member flexural response may be significantly influenced by joint detailing.

6.3 Repaired unit

1. Measured demand upon the specially-placed joint reinforcement of the repaired test unit allowed a validation of the prototype repair.

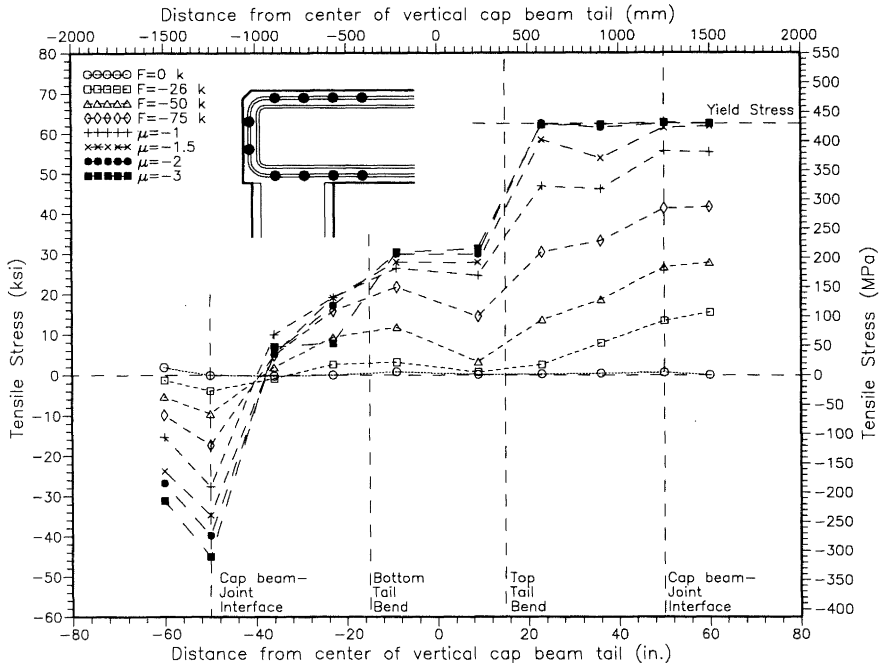

FIGURE 27 ***Closing-moment stress profiles along the embedded longitudinal cap beam reinforcement of the redesigned unit (see inset for location of gauges).***

2. Selecting the amount of required specially-designed joint reinforcement based upon criteria developed for building beam-column joints is unnecessarily conservative.
3. Cap beam plastic hinging at the joint interface should be avoided, particularly for sections with a comparatively low area of bottom longitudinal reinforcement.
4. Increasing the joint width is an effective method for reducing joint stress levels.
5. For joint-opening actions member reinforcement tension strains can be expected to penetrate into the joint.
6. Joint haunches effectively relocate plastic hinges further from the joint core, increase the reinforcement embedment depth, and modify the geometry of the joint diagonal strut.

6.4 Retrofitted unit

1. The use of prefabricated bolster cages resulted in an effective and simple external prestress retrofit scheme, improving joint-closing response and preventing cap beam

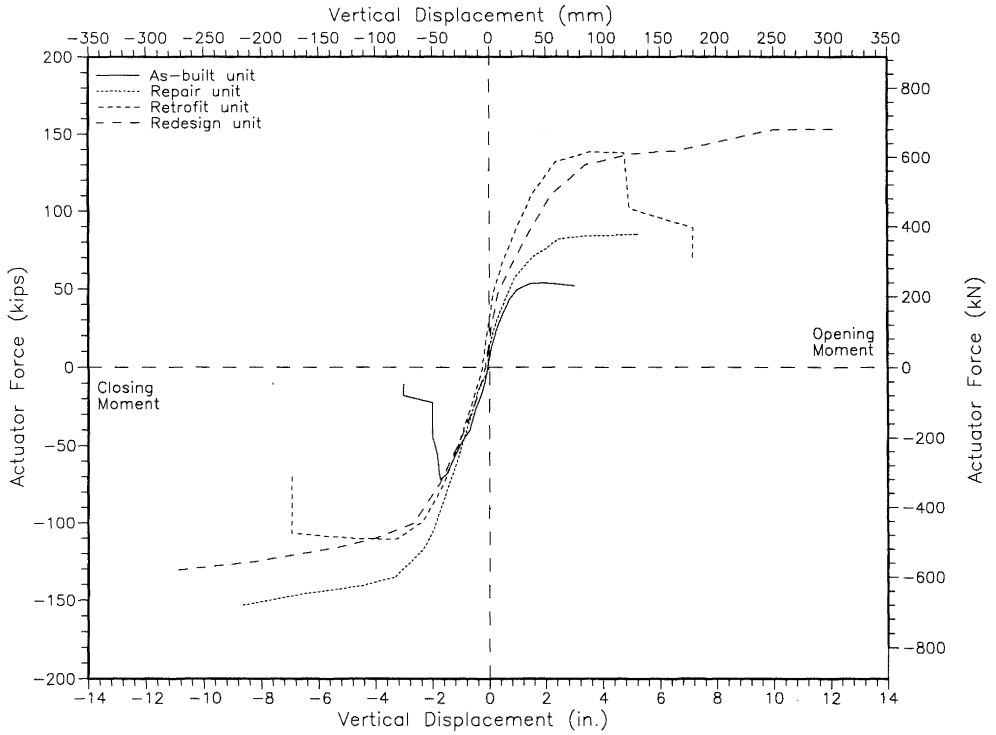

FIGURE 28 ***Force-displacement envelopes.***

plastic hinging.
2. To avoid joint strut crushing the maximum principal compression stress developed in effectively unreinforced bridge knee joints should not exceed $0.25 f_c'$, where f_c' is the actual or probable concrete strength, which is generally significantly greater than the design concrete strength.
3. Rational methods are available to assess the maximum capacity of struts in prestressed joints. Particular attention should be given to the capacity of the joint diagonal strut developed in bridge knee joints subjected to joint-opening actions.
4. Increasing the width of the retrofitted joint would have proportionally reduced the demand upon the joint diagonal strut, improving response.
5. Joint crack patterns and measured reinforcement strain data supported the assumed joint force transfer mechanisms.

6.5 Redesigned unit

1. The joint and cap beam redesign were successful in forcing plastic hinging into the column for both directions of loading, ensuring ductile inelastic deformation consistent with capacity design criteria.
2. Measured and targeted demand upon specially-placed joint reinforcement were in close agreement, supporting the design procedure.
3. Joint stress levels in excess of current US code recommendations can be supported when using rational design procedures.
4. Detailing of longitudinal member reinforcement embedded within the joint can have a significant influence upon the resulting joint force transfer mechanisms.
5. Extensive cracking and spalling of the cover concrete of well confined bridge knee joints does not significantly influence structural response.

ACKNOWLEDGEMENTS

This investigation was conducted in the Charles Lee Powell Structural Systems Laboratory at the University of California at San Diego, and the assistance of both the technical and undergraduate student staff of this facility is gratefully acknowledged. Funding for this investigation was provided by The California Department of Transportation (Caltrans).

REFERENCES

1. Ingham, J. M. 1995. *Seismic Performance of Bridge Knee Joints* Doctoral Dissertation, Department of Applied Mechanics and Engineering Sciences, University of California at San Diego, La Jolla, California, 502 p.

2. Bertero, V. V., and McGlure, G. 1964. *Behaviour of reinforced concrete frames subjected to repeated reversible loads*, ACI Journal, Vol. 61, No. 10, pp. 1305-1330.

3. Cote, P. A., and Wallace, J. W. 1994. *A study of reinforced concrete knee-joints subjected to cyclic lateral loading*, Report No, CU/CEE-94/04, Dept. of Civil Engineering, Clarkson University, N.Y., 143 p.

4. McConnell, S. W., and J. W. Wallace. 1994. *Use of T-headed bar in reinforced concrete knee joints subjected to cyclic lateral loading*, Report No. CU/CEE-94/10, Dept. of Civil Engineering, Clarkson University, N.Y. 44p.

5. Mazzoni, S., Moehle, J. P., and Thewalt, C. R. 1991. *Cyclic response of RC Beam-Column Knee Joints - Test and Retrofit*, Report No. UCB/EERC - 91/14, Earthquake Engineering Research Center, University of California at Berkeley, 24 pp.

6. Megget, L.M., and Ingham, J.M. 1996. *The Seismic behaviour of reinforced concrete beam-column knee joints for buildings*, Eleventh World Conference on Earthquake Engineering, Acapulco, Mexico.

7. Priestley, M. J. N., Seible, F., and Calvi, M. 1996. *Seismic design and retrofit of bridges*, John Wiley and Sons, New York, p. 686.

8. American Concrete Institute, 1992. *Building Code requirements for Reinforced concrete*, ACI 318-89 (Reapproved 1992), Detroit, Michigan.

9. AASHTO. 1989. *Standard specifications for Highway bridges*, Fourteenth edition, Washington D. C.

10. Standards New Zealand. 1995. *Concrete Structures Standard*, NZS 3101:Part 1 and 2:1995.

11. Housner, G. W. 1990. *Competing against Time:* Report to Governor George Deukmejian, The Governor's Board of Inquiry on the 1989 Loma Prieta Earthquake.

12. Thewalt, C. R., and Stojadinovic, B. 1995, *Behavior of Bridge Outrigger Knee Joint Systems*, Earthquake Spectra, Vol. 11, No. 3, pp. 477-509.

13. Priestley, M. J. N., and Seible, F. 1989. *Route 980, Bent #38 - A damage and repair assessment*, Final report to Caltrans office of Structures design, Department of Applied Mechanics and Engineering Sciences, University of California at San Diego, La Jolla, California.

14. Park, R., and Paulay, T. 1975. *Reinforced concrete structures*, John Wiley and Sons, New York.

15. Seible, F., and Priestley, N. 1990. *Damage and performance assessment of existing concrete bridges under seismic loads*, Proceedings of the First U.S.-Japan Workshop on Seismic Retrofit of Bridges, Tsukuba Science City, Japan, pp. 203-219.

16. Standards New Zealand. 1982. *New Zealand Code of Practice for the Design of Concrete Structures*, NZS 3101:1982 Part 1 and 2, Standards Association of New Zealand, Wellington.

17. Ingham, J. M., Priestley, M. J. N., and Seible, F. 1994. *Seismic Performance of Bridge Knee Joints - Volume 1*, Rectangular Column/Cap beam Experimental Results, SSRP-94/12, Department of Applied Mechanics and Engineering Sciences, University of California at San Diego, La Jolla, California.

18. Priestley, M. J. N. 1993. *Assessment and design of joints for single-level bridges with circular columns*, Report SSRP 93/02, Dept. AMES, University of California at San Diego, La Jolla, California.

19. Ingham, J. M., Priestley, M. J. N., and Seible, F. 1994. *Seismic Performance of Bridge Knee Joints - Volume 2*, Circular Column/Cap beam Experimental Results, SSRP-94/17, Department of Applied Mechanics and Engineering

Sciences, University of California at San Diego, La Jolla, California.

20. Tanaka, H., and Park, R. 1993. *Seismic Design and Behaviour of Reinforced Concrete Columns with Interlocking Spirals*, ACI Structural Journal, V. 90, No. 2, pp. 192-203.

APPENDIX A - LIST OF SYMBOLS

A_{bh} area of horizontal bolster reinforcement
A_{jh} area of horizontal joint reinforcement
A_{sb} area of beam reinforcement
A_s area of reinforcement
A_{sc} area of column reinforcement
C_b flexural compression force in beam
C_c flexural compression force in column
C_d diagonal compression force
D' diameter of core confined by circular hoops or spiral, measured to centreline of hoops or spiral
D_1, D_2 strut forces
F_h horizontal joint force
F_i seismic actuator force resulting in member ideal moment
F_y seismic actuator force resulting in member yield moment
f_r confinement stress
f_s reinforcement stress
f_y reinforcement yield strength
ℓ_a anchorage length
ℓ_s splice length
M_b beam moment
M_c column moment
M_i member ideal moment
M_y member yield moment
N_b beam axial force
N_c column axial force
p_c principal compression stress
p_t principal compression stress
p_x average joint horizontal compression stress
p_y average joint vertical compression stress
s reinforcement spacing
T_b flexural tension force in beam
T_c flexural tension force in column
T_{c1-3} components of column flexural tension force developed for joint-closing actions
T_{o1}, T_{o2} components of column flexural tension force developed for joint-opening actions
T_{ps} tension force in prestress tendons
T_s tension force in stirrups
V_b shear in beam
V_c shear in column
V_{jh} horizontal joint shear force
v_{jh} horizontal joint shear stress
v_{jv} vertical joint shear stress
v_j average joint shear stress
$\overline{x}$ distance to force centroid
Δ_y bilinear yield displacement
Δ_y' measured yield displacement
ε_{cu} ultimate concrete compression strain
ϕ strength reduction factor
ϕ_y bilinear yield curvature
ϕ_y' measured yield curvature
μ_f coefficient of static friction for concrete
μ_Δ displacement ductility level
ρ_s transverse reinforcement ratio